*Aust. J. Phys.*, 1976, **29**, 183–94

# A Long-range Ocean Radar for Ocean Surface Studies using Backscatter via the Ionosphere

*J. F. Ward*[A] *and P. E. Dexter*[B]

[A] Physics Department, James Cook University of North Queensland, Townsville, Qld 4811.
[B] Australian Bureau of Meteorology and Physics Department, James Cook University of North Queensland, Townsville, Qld 4811.

*Abstract*

An HF Doppler radar, designed for use at long range via an ionospheric propagation mode, has been developed primarily for the determination of wave states over large ocean areas. The operating frequency is 21·840 MHz, and the array is physically rotatable through a full 360° of azimuth, thus allowing for great flexibility in the choice of target area. The experimental technique utilizes a well-known resonance interaction mechanism for electromagnetic waves backscattered from a moving sea wave surface to derive sea state parameters in the scattering region for input to oceanographic and meteorological synoptic data networks. An ultimate angular resolution of less than 1° of azimuth, coupled with high operational flexibility, suggest possible utilization of the aerial array for tracking and interrogating free-floating ocean buoys, tracking radio noise associated with tropical cyclones and investigating aspects of ionospheric dynamics.

## 1. Introduction

The study of HF radar backscatter echoes from rough ocean profiles as a possible method for the remote determination of surface wind conditions is of considerable interest in radio physics, oceanography and synoptic meteorology. Crombie (1955) demonstrated the existence of such ocean echoes and gave a simple interpretation. His work was extended from a short-range surface-wave propagation path over the sea to a long-range ionospheric mode of one or more hops by Ward (1969), who achieved successful power spectra analyses for data at Townsville (latitude 19·25° S., longitude 146·74° E.) that were derived from ocean regions south of Hobart: a range of approximately 2800 km. Although the fixed array used in these early experiments had a beam which could be slewed electrically over a small arc, it became clear that flexibility in selection of ocean targets was a prime requirement for further progress. As a result, a major coherent radar installation operating at 21 MHz was designed and set in operation at Townsville by the James Cook University and was officially commissioned by the Director of the Australian Bureau of Meteorology in 1973.

An extensive experiment of over one year duration, essential to the design, was carried out in 1971–72 to study typical ionospheric dynamics in relation to phase path instability. This yielded one parameter in the specification of performance possible in the radar (Ward 1972). Besides specific observations of target regions of interest in various oceans surrounding Australia, a series of systematic observations of the Tasman Sea between Auckland and Sydney was undertaken. Some results were presented by one of us (J.F.W.) to the URSI Symposium at Warsaw, Poland, in 1972 and contributed to the URSI Symposium at Lima, Peru, in 1975. The broad

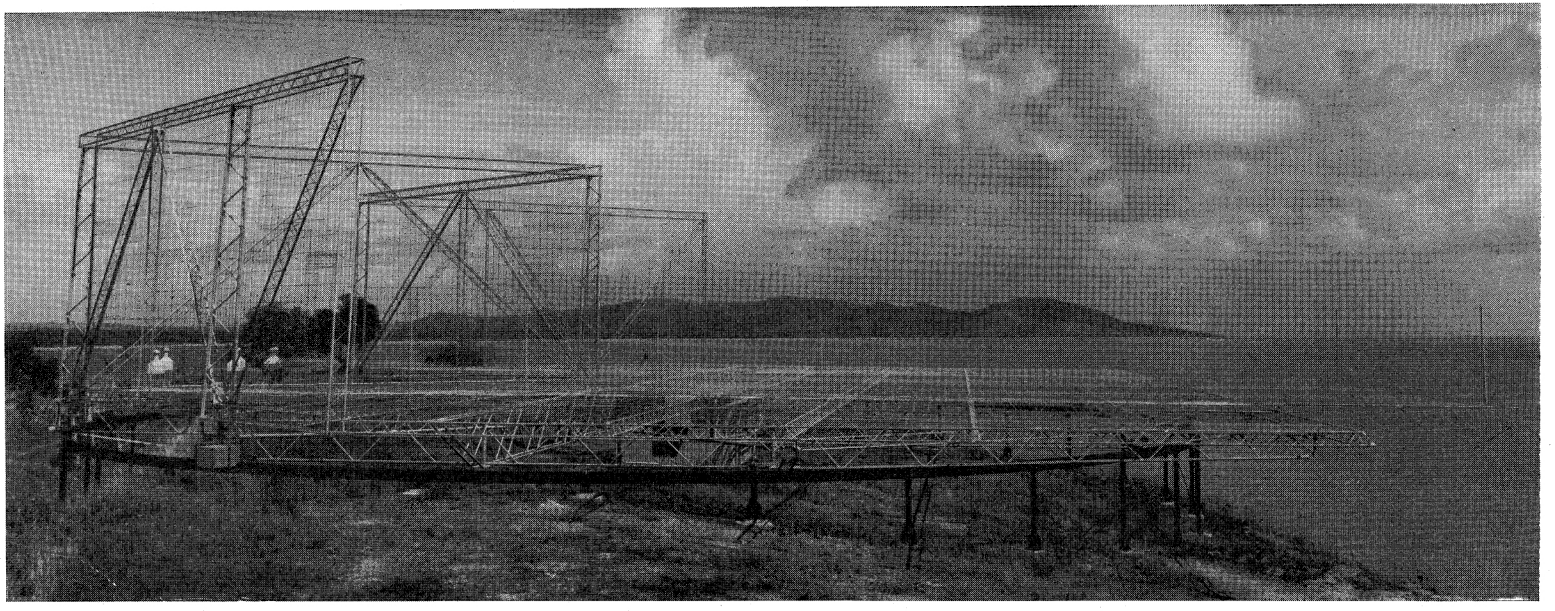

**Fig. 1** (*above*). General appearance of the long-range HF ocean radar at Townsville.

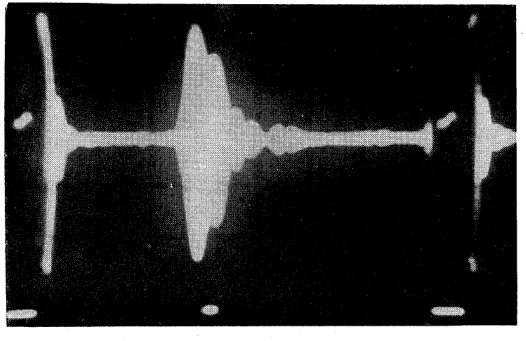

**Fig. 2** (*left*). A typical A scan sea-echo group, with amplitude-limited transmitted pulse for timing. The repetition period is 40 ms. Gating samples are indicated in the lower trace.

object of the study now in progress is to designate the degree of correlation between accurately known ocean conditions and the sea state as derived at a remote location by the radar probing and analysis. The approach adopted in this work is outlined together with some typical results in Section 4.

## 2. Experimental Facility

The operating frequency of the radar of 21·840 MHz ($\lambda_r$ = 13·8 m) was chosen to be as high as the *F* layer would sustain for oblique modes during daylight hours when the normal ionosphere was expected to be in its most stable condition. A compromise between propagation needs and aerial directivity had to be made.

For resonance with the ocean-wave backscattering region, a sea wavelength $\lambda_w$ of $0{\cdot}5\lambda_r$ (6·9 m) was thus necessary. This yields the Bragg resonance line in the spectrum (Crombie 1955), as is discussed in Section 4 below. Reasonable aerial directivity and gain could be expected for the physical dimensions thus imposed, but the consequent value of $\lambda_w$ is shorter than that for the peak in the energy–wavelength spectrum of a fully developed wind-driven ocean wave system (Phillips 1966). Experiment has shown, however, that adequate return signals can be attained to meet the needs of the extremely narrow band detection systems used in the coherent radar.

The aerial array consists of an interferometry pair of two sets of unbalanced monopoles which excite (as distributed feeds) two large corner reflectors ($3{\cdot}0 \times 0{\cdot}5\lambda$). The design configuration was optimized by model studies at 1000 MHz, and the resultant H.F. radar version was scaled up by 50 : 1 to operate at 21 MHz. The array (see Fig. 1) is based on the very much larger low-delta designs studied and constructed by Ward (1965*a*, 1965*b*, 1965*c*). With its associated earth plane, this version is completely rotatable in azimuth, with a setting accuracy of $\pm 0{\cdot}25°$ and a final bearing accuracy of $\pm 0{\cdot}5°$. A gondola carrying the high-power radar transmitter and ancillary controls is suspended below the earth plane to rotate integrally with it. The moving structure weighs approximately 20 tonne and can traverse 360° of azimuth very smoothly in 3 min. The cliff top location of the station was chosen to give unobstructed sea horizons in all directions of interest, so that near-grazing angles of fire and reception would permit single-hop *F*-layer ionospheric propagation modes with ranges approaching the 4000 km theoretical limit. Studies at UHF (Thiel 1973) have indicated modifications which could be applied to adjust the vertical (*E*) plane polar-pattern if the sea ray interference due to the cliff height of $2\lambda$ above the sea proved to be troublesome for some target ranges of particular interest. In practice this has been found unnecessary, and all ranges from the skip distance out to about 4000 km appear to be attainable in the first-hop mode. Echoes from two-hop paths out to 6000 km have been noted, and enough coherence has been found within these to warrant further study later. A typical A scan portrayal showing sea echoes suitable for analysis is given in Fig. 2.

The azimuthal (*H*) plane polar-pattern of the array is shown in Fig. 3. It indicates the usual design compromise between beamwidth ($\pm 12°$ for 3 dB) and interferometric side lobe level. As the radar operates in the monostatic mode by means of a TR aerial switch, an effective side lobe suppression of the order of 15 dB with respect to the main lobe is attained operationally, and this is found to be adequate to ensure that the phase coherence of the overall system is controlled by the energy received within the main beam only. As the receiving processing equipment utilizes phase lock procedures with long electrical time constants, there is evidence that the final

coherence is achieved by the time-statistics of the strongest echo contributions. This means that the effective dynamic beamwidth of the array may be narrower than that based on the 3 dB criterion, as quoted above. This dynamic property improves resolution in both the range and azimuth dimension. The particularly high front-to-back ratio of approximately 20 dB is an important operational feature of the array, for which the forward gain is $13 \pm 1$ dB with respect to a free space dipole. When out-phasing is applied within the main lobe of the interferometric pattern it gives a null which is useful for direction-finding purposes to yield an angular resolution of much

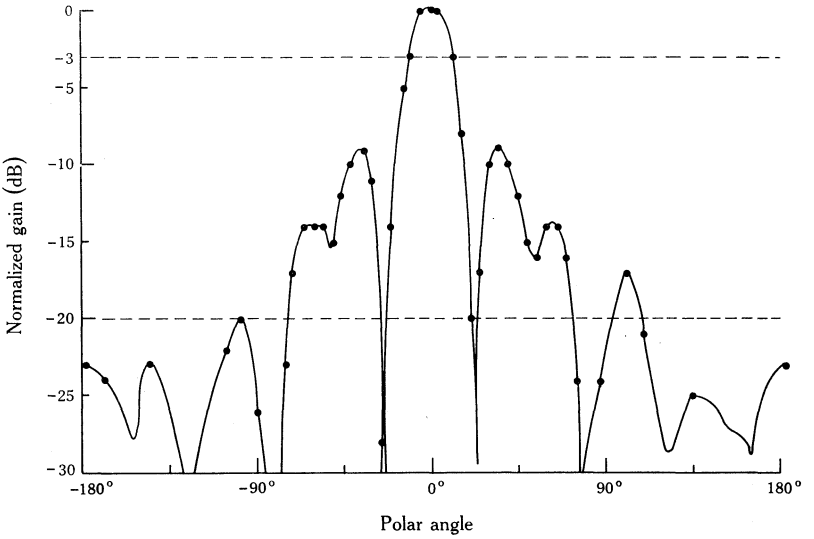


**Fig. 3.** *H* plane polar diagram of the HF radar for an elevation angle of 8°. The r.m.s. error is $\pm 0{\cdot}6$ dB.

less than 1° of azimuth. When driven with a transmitter of output 20 kW peak pulse power, the field strength measured by one of us (J.F.W.) at Singapore in December 1972 was comparable with that of Radio Australia, Radio Cologne and the Voice of America; all of which were on adjacent frequencies. The effectiveness of the array in a possible short wave broadcast role to achieve service areas by one- or two-hop modes for any chosen azimuthal direction is obvious. In the radar mode the present transmitter with the array can yield an effective radiated power of up to $0{\cdot}5$ MW. Pulse lengths of $0{\cdot}5$–$1{\cdot}0$ ms duration and repetition periods of 40 or 80 ms are available.

Owing to flexibility in the choice of the region of ionosphere to be illuminated, the coherent radar is a very useful instrument for studying the dynamics of the ionosphere as such and, in particular, for performing morphological studies of travelling ionospheric disturbances (experiments of this kind are currently being carried out). In conjunction with the Bureau of Meteorology, we have used the array in simulated experiments on the tracking and interrogating of free-floating instrumented buoys. The array is also being used to study the morphology of ionospherically propagated HF radio noise at about 20 MHz associated with selected equatorial regions. Interesting results have been obtained from the tracking of distant tropical cyclones by virtue of their generation of significant localized radio noise in a band capable of ionospheric propagation. An idea of the performance of the extremely

narrow-band coherent equipment when used to detect and study the sea echoes can be gained from Fig. 4 (below). These records are for a target in the Tasman Sea out to 3500 km from Townsville, and were taken under quiet ionospheric conditions when the local time at the reflection region was near 1400 h.

The optimum times for using the ionosphere as part of the transmission path in an extended-range coherent radar have been determined diurnally and seasonally by Ward (1972) from a sustained series of phase path measurements, which yielded statistical data based on more than 2000 separate Doppler frequency measurements extending over an observation time of more than one year. The resolution limit imposed by the dynamics of the ionosphere is predicted from this ancillary experiment to be $\pm 0{\cdot}01$ Hz. Ideally, during radar probing, there should exist a means to monitor independently the phase path fluctuations introduced by the ionosphere at the reflection regions in the latitudes of interest. Aberrations due to travelling ionospheric disturbances could then be excluded or minimized.

Correction for phase perturbations introduced by multi-path modes in the propagation path can be carried out effectively in the signal processing equipment by electronic logical decisions based on both the fade depth and the rate of fade parameters. This is a form of electronic editing of the data in real time. For observational samples of duration 100 s or more, however, the spectral analysis operation applied to the data tends to minimize this problem by suppressing the perturbations and thereby lowering the background phase 'noise'.

The amplitude–time analogue output from the synchronous detector contains contributions from all Doppler phase shift components in the incoming echo signal. The processing of this signal is outlined in the next section. A second phase-sensitive detector yielding a ramp-function output is used to indicate, by the positive or negative gradient of the ramp, the sense of the Doppler frequency shift, i.e. decreasing or increasing.

As a result of this type of data processing, spectral lines can be resolved to at best the limit of $\pm 0{\cdot}01$ Hz imposed by the instability of the propagation medium when conditions are near to ideal. Such a result for the 21 MHz irradiation frequency corresponds to a measurement of Doppler shift to approximately $\pm 5$ parts in $10^{10}$. Data taken from successive azimuthal bearings in the form of arc samples of 10°–20° and for radar ranges in increments of about 150 km (as determined by the choice and gating-out of viewing samples with different propagation times for selected target regions) comprise the basis for the computation and subsequent derivation of a matrix of target conditions leading to ocean surface predictions of meteorological significance (Tvetven 1967; Ward 1969; Earl 1971; Hasselmann 1971; Dexter 1972, 1973; E. D. R. Shearman, personal communication). This is discussed in Sections 3 and 4 below. Thus, for an observationally quiet period of about 2 h per day, it is expected that about 100 observation regions could be probed and that spectra from these could be produced within 2–4 h of the time of measurement to make available for meteorological interpretation a significant matrix of ocean data almost in real time.

## 3. Spectral Analysis

The principal method of data collection currently employs magnetic tape as a means of temporary data storage, although this stage could be eliminated in future by introducing on-line data processing. The time-dependent phase–amplitude data,

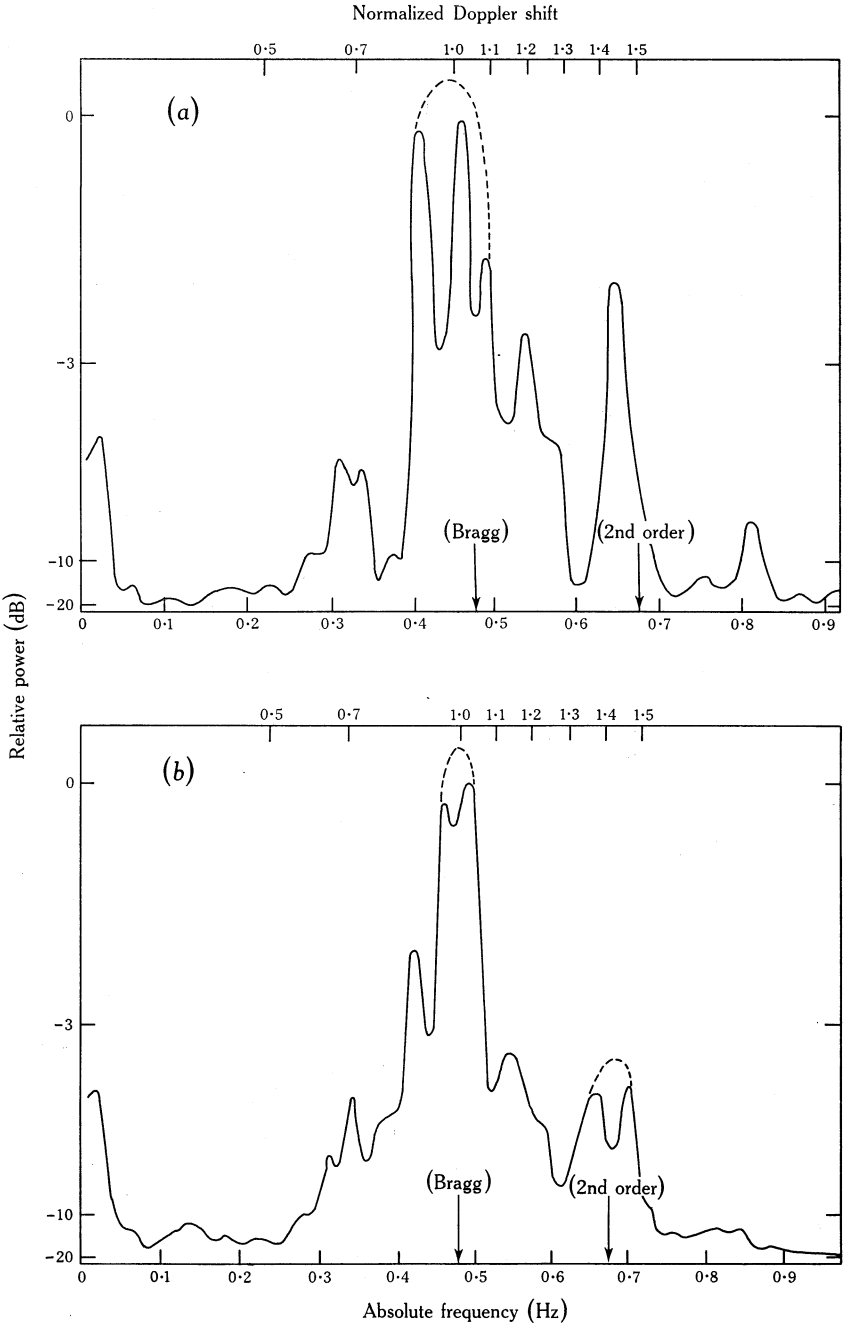


**Fig. 4.** Normalized smoothed Doppler spectra for data recorded near 1420 h local time on 28 October 1974 with the HF radar. The scattering is from an area of sea at a total time-of-flight range of 24 ms on a radar bearing of 170° true. The expected Bragg and second-order peak locations are indicated.

(*a*) Data are for a single 100 s block. Computer derived points were plotted every 0·01 Hz and the curve was then interpolated manually.

(*b*) Data are for five 100 s blocks, including that used in (*a*).

in the form of a time-varying DC signal (low pass filtered to 1 Hz), is used to frequency modulate a signal up to 10 kHz, and the result is then passed to the magnetic tape. Subsequent decoding back to the time-varying DC signal (0–10 V) is necessary before digitization can be effected with a PDP-8S minicomputer system. A sample interval of 0·1 s is used, and blocks of 100 s length are thus converted to give time series of 1000 data points each.

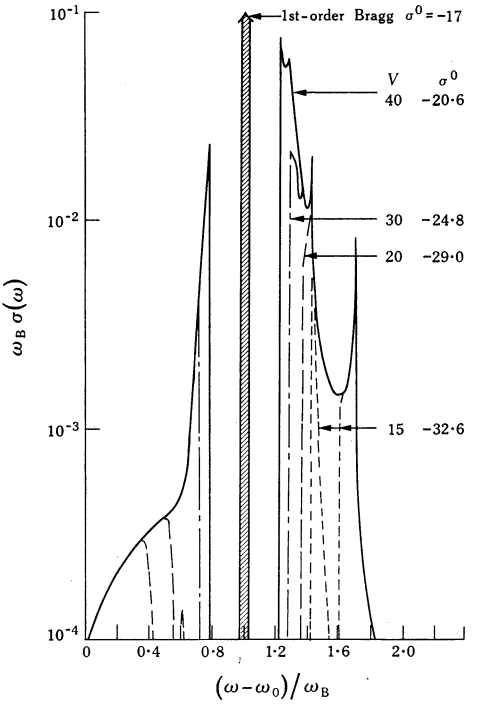


**Fig. 5.** Predicted normalized backscatter cross section $\omega_B \sigma(\omega)$ as a function of the normalized Doppler shift $(\omega-\omega_0)/\omega_B$, showing first- and second-order near-grazing sea backscatter at 10 MHz for propagation in an upwind direction. A Phillips semi-isotropic waveheight spectrum is assumed. The wind velocity $V$ (knots) and the average scattering cross section $\sigma^0$ (dB) of the sea per unit area are given. (The theoretical spectrum shown here follows Barrick 1972*b*.)

Spectral analysis is carried out on a larger PDP-10 system using, at present, a simple periodogram technique to compute the power of the first 100 Fourier components, with a spectral resolution of 0·01 Hz in the range 0–1 Hz. Aliasing is avoided through the use of the low pass filter mentioned above. Smoothing is effected with a hanning window, and the spectral ordinates are finally normalized to the maximum value before output. Incoherent averaging is performed simply by averaging the unsmoothed spectral ordinates of spectra recorded in the same time block and representing the same radar range and bearing, with the smoothing and normalization then applied as before. Examples of power spectra computed in this way are shown in Fig. 4*a*, which is the spectrum for a single 100 s data block, and in Fig. 4*b*, which is the result of averaging five spectra incoherently (including that of Fig. 4*a*). The vertical axes are labelled in decibels below the maximum value, while the lower horizontal axis gives the absolute frequency and the upper horizontal axis gives the frequency normalized to that of the maximum spectral line.

## 4. Theory and Interpretation

In recent years the theory of the scattering of electromagnetic waves of various frequencies from rough water surfaces has become relatively well known. In particular,

explicit formulations for the scattering cross section, to both first and second order, have been derived in terms of various assumed water wave spectra. At MF and HF radio frequencies, the best solutions are obtained using a boundary perturbation technique based on the generalized analysis by Rice (1951), and details of this approach may be found in the works of Crombie (1971), Hasselmann (1971) and Barrick (1972*a*, 1972*b*). A physical optics technique is also available, and has been shown by Dexter (1973) to give similar results for radar observations in the upper HF frequency range and at near-grazing incidence. However, it is generally less applicable than, and is considered to be inferior to the former approach.

The interaction between radio waves and ocean wave trains is conceived theoretically in terms of the latter appearing as a diffraction grating, with various orders of interaction explainable in terms of Bragg scatter. To first order, the average backscatter cross section per unit area per unit (rad $s^{-1}$) bandwidth, for grazing incidence and vertical polarization is given by (e.g. Barrick 1972*b*)

$$\sigma(\omega) = 2^7 \pi k_0^4 S(K_x, K_y)\, \delta(\omega - \omega_0 \pm (2gk_0)^{\frac{1}{2}}), \tag{1}$$

where $k_0$ and $\omega_0$ are the wavenumber and frequency of the incident radiation, $S(K_x, K_y)$ is the spatial waveheight directional spectrum of the sea surface, $\omega$ is the radio frequency of the scattered radiation and $g$ is the gravitional acceleration. It is a consequence of this equation that energy peaks will exist in the backscatter signal at frequencies

$$\omega = \omega_0 \pm (2gk_0)^{\frac{1}{2}} = \omega_0 \pm \omega_B, \tag{2}$$

which correspond to Doppler frequency shifts imposed by water waves of wavelength $L = \frac{1}{2}\lambda_r$ (where $k_0 = 2\pi/\lambda_r$) moving radially towards or away from the radar, thus conforming to the original empirical deductions of Crombie (1955).

The extension of the theory to second-order analysis is straight forward, although the backscatter cross section then becomes more complex, involving interactions between the incident radio wave and two water wave trains. In such a case, peaks in the backscatter spectrum should occur at frequencies

$$\omega = \omega_0 \pm (g\,|\,\boldsymbol{K}_1\,|)^{\frac{1}{2}} \pm (g\,|\,\boldsymbol{K}_2\,|)^{\frac{1}{2}}, \tag{3}$$

where $\boldsymbol{K}_1$ and $\boldsymbol{K}_2$ are the spatial wavenumbers of the water wave trains. Only the resultant of the two ocean wave vectors $\boldsymbol{K}_1$ and $\boldsymbol{K}_2$ needs now to be aligned radially to the radar, and so waves of significant energy propagating at various angles to the radial direction may contribute to the second-order spectrum. Physically, two particular contributions to this second-order spectrum have been identified: (1) an electromagnetic effect, in which an ocean wave train $\boldsymbol{K}_1$ scatters radio energy along the surface to train $\boldsymbol{K}_2$ which redirects it back to the receiver; (2) a nonlinear hydrodynamic effect, in which $\boldsymbol{K}_1$ and $\boldsymbol{K}_2$ combine to produce second-order (real but not freely propagating) ocean waves $\boldsymbol{K}_1 \pm \boldsymbol{K}_2$, which in turn generate backscatter with different and predictable Doppler shifts.

The identification and interpretation of the first-order (Bragg) peaks in the Doppler frequency spectrum of the backscatter signal have been well established since the time of Crombie (1955). Indeed, in principle, these would be sufficient to measure the total sea wave energy spectrum through the inversion of equation (1), provided the radar frequency could be altered at will so as to determine $\sigma(\omega)$ over a sufficient

range of frequencies. Unfortunately this approach is impracticable because of the physical limitations on radar design, which are especially restrictive for ionospheric propagation modes, where considerable directionality is required and for which radio frequencies from 1–30 MHz would be necessary to cover a normal sea wave spectrum. A further difficulty for radar systems operating in the upper HF region concerns the fact that the sea waves producing first-order scatter will be 'saturated' for most wind speeds. This means that the amplitude of the Bragg peak will be invariant over a wide range of sea conditions (e.g. at 21·8 MHz, saturation of the waves producing Bragg scatter occurs at a surface wind speed as low as 4 m $s^{-1}$). Under these conditions, information on the full ocean wave spectrum must be sought in the higher-order terms in the backscatter spectrum.

Following the observation of second-order sidebands displayed in the experimental spectra of Ward (1969), interpretations have been advanced by Hasselmann (1971), Crombie (1971) and Barrick (1972*b*). Again, while it is theoretically possible to invert the equation for the backscatter cross section (this time at a single radio frequency) in order to obtain the complete sea wave spectrum, it has been found more practical to substitute an assumed ocean spectrum into the equation and compare the results with the observed Doppler spectra. It is apparent from equation (3) that there should be present in the Doppler spectrum second-order sidebands arrayed around the Bragg peak. Both theory and observation show that these second-order peaks will vary in magnitude and proximity to the Bragg peak as a function of the surface wave field (or, more simply, as a function of the significant waveheight $H_s$, defined as the average height of the highest one-third of all waves). Two particular second-order peaks will frequently be evident, located at frequencies $2^{\frac{1}{2}}$ and $2^{\frac{3}{4}}$ times the shift of the Bragg peak and with amplitudes dependent on $H_s$.

Using theoretical computations of Doppler spectra based on a Phillips (1966) model for the sea surface, Barrick (1972*b*) and Barrick *et al.* (1974) were able to identify a parameter $\beta \approx 10\omega_0 H_s/c$, which may be used in relating the amplitude of the second-order sidebands to the significant waveheight for a fixed radar frequency $\omega_0$. They have supported their theory with observations made using a surface-wave propagation mode, in which some 30 min of data were averaged to obtain each Doppler spectrum. Unfortunately, the range of observation and the amount of useful data it is possible to collect are very limited in such experiments though it is of interest to note that similar short-range observations have been made by various Russian workers for some time now (e.g. Braude *et al.* 1962).

The determination of details of the second-order spectrum for backscatter using an ionospheric propagation mode is considerably more difficult than for surface wave propagation, because of the uncertainties introduced by moving ionospheric layers. While it seems likely (Crombie 1971; Barrick 1972*b*) that ionospheric Doppler shifts will normally be manifested as displacements of the first-order peak from its theoretical position, these must inevitably lead to the broadening of the Bragg peak and to uncertainties in the position and magnitude of the secondary spectral peaks as longer periods of data are included in deriving each spectrum. Attempts by Long and Trizna (1973) and Ahearn *et al.* (1974) to overcome this problem have involved the use only of the two (positive and negative Doppler frequencies) first-order Bragg peaks and the neglect of higher-order details. This approach relies on empirical relationships which are themselves subject to considerable uncertainty, particularly

for complex sea surface conditions. In addition, a two-sided Doppler spectrum is not presently available from the James Cook system, and we thus have to rely on an examination of the second-order peaks. In this circumstance, a satisfactory spectral determination will represent a balance between the long record lengths required for a proper definition of higher-order detail, and the increasing ionospheric uncertainties as observation time and averaging increase. At present, a record length of some 8 min (made up of five 100 s data sets) seems to be the best compromise, but further tests are being carried out to confirm this.

The spectra presented in Fig. 4 should be examined in the light of the above comments. The data were recorded at 1420 h local time on 28 October 1974, on the radar bearing of 170° true, and at a total time-of-flight range of 24 ms. This places the scattering area 800 km to the SSE. of Tasmania, where the seas had been generated for some 36 h by a NW. airstream of up to 15 $m\,s^{-1}$ ahead of an approachng cold front. Thus significant waveheights of up to 6 m could be expected, with most of the wave energy moving away from the radar and contained in wave periods around 11 s.

A total of some 20 min of the phase–amplitude–time signal for this scattering location was recorded on both magnetic tape and strip chart, and a power-spectral analysis was performed on each 100 s block of the digitized data. The spectra were then smoothed and finally averaged incoherently in groups of 3, 5 and 11. The resulting Doppler power spectra are those shown in Figs 4*a* and 4*b* (above). For comparison, a theoretical spectrum (taken from Barrick 1972*b*) for an assumed Phillips (1966) model sea is shown in Fig. 5. The second-order peaks in Fig. 5 are associated (as indicated) with the following wind velocities: 40, 30, 20 and 15 knots (corresponding to 20·6, 15·4, 10·3 and 7·7 $m\,s^{-1}$). The quantity $\sigma^0$ is the average scattering cross section of the sea per unit area, and is given by (Barrick)

$$\sigma^0 = \tfrac{1}{2}\int_{-\infty}^{\infty} \sigma(\omega)\,\mathrm{d}\omega .$$

The most important features of these results include:

(1) The resolution of the Bragg peak has improved considerably from Fig. 4*a* to 4*b*, and the level of the background noise has dropped as a result of the incoherent averaging, i.e. due to the suppression of ionospheric phase path fluctuations. Although not shown here, it is worth noting that the level of ionospheric noise increased considerably for data blocks after the fifth (the last of the blocks contributing to Fig. 4*b*), and this led to an increased uncertainty in the frequency of the first-order peak, together with an almost complete masking of the second-order sea effects. This feature has been apparent in a number of records and forms the basis for the earlier statement that, for the radar and paths under discussion, approximately 8 min of recorded data represents the best compromise for analysis purposes.

(2) A distinct second-order peak located at the expected frequency ($2^{\frac{1}{2}}$ times the Bragg frequency, the latter being 0·475 Hz for a 21·840 MHz radar) is evident in both spectra, being probably more significant in terms of general noise levels in Fig. 4*b*. Certainly the amplitude of the second-order peak relative to the Bragg peak is more easily estimated in the averaged spectrum, owing to the improved resolution and significance of both peaks. This is an essential feature if estimates of the sea state are to be made.

(3) Only a small shift is evident in the position of the Bragg peak from its expected location at 0·475 Hz. This shift is of order 0·01 Hz in both spectra and approaches the resolution limit of the experimental analysis, indicating the presence of little net ionospheric movement during the recording period. The reverse is true for later records in this group (as mentioned above), for which ionospheric motions were obviously large and irregular.

Since seas in the scattering region would have been close to their fully developed state for an average wind speed of 15 $m\,s^{-1}$, some limited comparison may be made with Barrick's (1972*b*) theoretical results, which are shown in Fig. 5. For a 15 $m\,s^{-1}$ wind, his theory gives a secondary peak at a normalized frequency of 1·414 (i.e. $2^{\frac{1}{2}}$ times the Bragg peak), with amplitude −7·8 dB with respect to the Bragg peak. For a 20 $m\,s^{-1}$ wind, the expected amplitude is −3·6 dB. An estimate from Fig. 4*b* puts the experimental level at about −5 dB, which is a very reasonable comparison at this stage, considering the uncertainties that are associated with both theory and experiment.

## 5. Future Work

While the potential of both the general approach to remote sensing of sea states at great distances and the particular experimental facility of the James Cook University is obvious from the present results, there seems little doubt that the major limiting factor in its practical application is the presence of ionospheric noise in the Doppler spectra. However, in order to determine exactly the limitations imposed, experimental derivations must be made of sea Doppler spectra in the absence of the noise, and comparisons then made with actual sea spectra. This may be done in two ways: (1) by using only surface-wave backscatter with HF radars (e.g. Crombie 1971; Barrick *et al.* 1974); (2) by exploiting the analogy which exists between the scattering from a water surface of sound waves in air and of electromagnetic waves (Dexter 1972).

In an earlier relatively simple experiment, one of us (P.E.D.) scattered ultrasonic waves of frequency 40 kHz from a capillary-wave water surface, and established the broad validity of the first-order theory, as well as determining possible angular effects. To obtain a more detailed elucidation, this experiment has now been redesigned in order that precise measurements may be made of both water wave spectra directly (using a capacitance probe for wind-generated capillary waves in a tank) and of the corresponding spectra derived from the backscatter process. Results from this experiment are now being analysed and will be published separately.

## Acknowledgments

The support of the Australian Bureau of Meteorology and the Radio Research Board has been essential to the evolution and commissioning of this major national facility. The Australian Army cooperated by making available the excellent site with good sea aspect in the Kissing Point Army Barracks, Townsville. The advice of Dr M. L. Heron, particularly on data analysis and interpretation, was greatly appreciated. One of us (P.E.D.) has had the assistance of an Australian Government Service Scholarship during part of the research.

## References

Ahearn, J. L., Curley, S. R., Headrick, J. M., and Trizna, D. B. (1974). *Proc. IEEE* **62**, 681–7.
Barrick, D. E. (1972*a*). *IEEE Trans. Antennas Propag.* **10**, 2–10.
Barrick, D. E. (1972*b*). *In* 'Remote Sensing of the Troposphere' (Ed. V. E. Derr), Ch. 12 (U.S. Govt: Washington, D.C.).
Barrick, D. E., Headrick, J. M., Bogle, R. W., and Crombie, D. D. (1974). *Proc. IEEE* **62**, 673–80.
Braude, S. Ya., Men', A. V., Poplavko, Yu. V., Turgenev, I. S., Shul'ga, V. F., and Lebedeva, O. M. (1962). *In* 'The Radioceanographic Investigation of Sea Swells' (Ed. S. Ya. Braude), pp. 58–97 (English translation) (Acad. Sci. Ukrainian SSR: Kiev).
Crombie, D. D. (1955). *Nature* (*London*) **175**, 681–2.
Crombie, D. D. (1971). *In* 'Electromagnetic Probing in Geophysics' (Ed. J. R. Wait), Ch. 4 (Golem: Boulder, Colorado).
Dexter, P. E. (1972). *Aust. J. Phys.* **25**, 419–28.
Dexter, P. E. (1973). M.Sc. Thesis, James Cook University.
Earl, G. F. (1971). Ph.D. Thesis, University of Melbourne.
Hasselmann, K. (1971). *Nature Phys. Sci.* **229**, 16–17.
Long, A. E., and Trizna, D. B. (1973). *IEEE Trans. Antennas Propag.* AP **21**, 680–5.
Phillips, O. M. (1966). 'Dynamics of the Upper Ocean' (Cambridge Univ. Press).
Rice, S. O. (1951). *In* 'Theory of Electromagnetic Waves' (Ed. M. Kline), pp. 351–78 (Interscience: New York).
Thiel, D. V. (1973). M.Sc. Thesis, James Cook University.
Tvetven, L. (1967). *Science* **157**, 1302.
Ward, J. F. (1965*a*). *Nature* (*London*) **205**, 1062.
Ward, J. F. (1965*b*). *Electron. Lett.* **1**, 195.
Ward, J. F. (1965*c*). *Trans. Inst. Eng. Aust.* EE **1**, 117.
Ward, J. F. (1969). *Nature* (*London*) **223**, 1325–30.
Ward, J. F. (1972). Phys. Dept James Cook Univ. Res. Rep. No. 23.

Manuscript received 8 December 1975